Dalton Transactions

Cite this: *Dalton Trans.*, 2012, **41**, 11753

www.rsc.org/dalton

PAPER

Incorporation of triazole into a quinoline-rhodamine conjugate imparts iron(III) selective complexation permitting detection at nanomolar levels†

Narendra Reddy Chereddy,[a] Sathiah Thennarasu*[a] and Asit Baran Mandal*[b]

Received 19th June 2012, Accepted 26th July 2012
DOI: 10.1039/c2dt31316b

Two new rhodamine based probes **1** and **2** for the detection of Fe^{3+} were synthesized and their selectivity towards Fe^{3+} ions in the presence of other competitive metal ions tested. The probe **1** formed a coloured complex with Fe^{3+} as well as Cu^{2+} ions and revealed the lack of adequate number of coordination sites for selective complexation with Fe^{3+}. Incorporation of a triazole unit to the chelating moiety of **1** resulted in the probe **2**, that displayed Fe^{3+} selective complex formation even in the presence of other competitive metal ions like Li^{+}, Na^{+}, K^{+}, Cu^{2+}, Mg^{2+}, Ca^{2+}, Sr^{2+}, Cr^{3+}, Mn^{2+}, Fe^{2+}, Co^{2+}, Ni^{2+}, Zn^{2+}, Cd^{2+}, Hg^{2+} and Pb^{2+}. The observed limit of detection of Fe^{3+} ions (5×10^{-8} M) confirmed the very high sensitivity of **2**. The excellent stability of **2** in physiological pH conditions, non-interference of amino acids, blood serum and bovine serum albumin (BSA) in the detection process, and the remarkable selectivity for Fe^{3+} ions permitted the use of **2** in the imaging of live fibroblast cells treated with Fe^{3+} ions.

Introduction

Iron is an essential trace element for both plants and animals, and plays an important role in cellular metabolism[1] and enzyme catalysis.[2] In humans, Fe^{3+} acts as the oxygen carrier in haemoglobin and a cofactor in many enzymatic reactions involved in the mitochondrial respiratory chain.[2a] Consequently, Fe^{3+} deficiency leads to anemia, liver and kidney damages, diabetes, and heart diseases.[3] Therefore, selective detection of Fe^{3+} has assumed importance in recent years. Both qualitative and quantitative techniques like atomic absorption spectroscopy,[4] colorimetry,[5] spectrophotometry,[6] and voltammetry[7] have been used for the detection of Fe^{3+} ions. But these require sophisticated equipment, tedious sample preparation procedures and trained analysts. Therefore, probes which allow naked-eye detection, have advantages over other methods in being easy to operate, portable, and not requiring sophisticated instrumentation.

The metal ion Fe^{3+} is a fluorescence quencher because of its paramagnetic nature.[8] Therefore, development of probes that exhibit fluorescence enhancement upon binding with Fe^{3+} would be very attractive. Although several probes have been reported in the literature for Fe^{3+} detection,[9–11] some of the probes developed for selective detection of Fe^{3+} suffer from cross-sensitivity towards competitive metal ions like Cu^{2+} and Cr^{3+}.[11] Hence, a probe that detects Fe^{3+} selectively, even in the presence of other competitive metal ions would be more attractive. As the availability of metal specific chelating moieties is limited, chemical modification of the available ligands for the selective complexation with the metal ion of interest is attaining importance.[11a,12]

8-Hydroxyquinoline is one of the widely used chelating moieties for metal ion coordination, and quite a number of chemically modified 8-hydroxyquinoline derivatives have been used as metal binding probes.[13] But, the major drawbacks of these probes are their photo physical properties in the far UV region, low quantum yield, and high solvent dependent fluorescence characteristics. Rhodamine is one of the most attractive fluorochromes available because of its photo physical properties such as high quantum yield, photo stability, and absorption and emission in the visible region.[14] Recently, much effort has been focussed on the development of rhodamine based probes for the detection of heavy metal ions.[15]

Recently, Zeng's group reported a rhodamine–quinoline conjugate with 'O–N–N' metal chelating moiety as a fluorescent sensor for Cu^{2+} ions, without interference from its competitive metal ions.[16] In the present work, we have explored the effect of additional coordinating moieties to tune the selectivity from Cu^{2+} to Fe^{3+} ion. We synthesized two rhodamine conjugates **1** and **2** containing 8-hydroxyquinoline and 8-((1-benzyl-1*H*-1,2,3-triazol-4-yl)methoxy)quinoline, with 'O–N–N–O' and 'O–N–N–O–N' combination of chelating moieties, respectively. The sensitivity and selectivity of **1** and **2** for the detection of Fe^{3+} in the presence of other competing metal ions were established. The stability and fluorescence characteristics of **2** in physiologically relevant conditions were exploited for the detection of live fibroblast cells exposed to Fe^{3+} ions.

[a]*Organic Chemistry Division, CSIR-Central Leather Research Institute, Adyar, Chennai-600 020, India. E-mail: thennarasu@gmail.com*
[b]*Chemical Laboratory, CSIR-Central Leather Research Institute, Adyar, Chennai-600 020, India. E-mail: abmandal@hotmail.com*

†Electronic supplementary information (ESI) available: $^{1}H/^{13}C$ NMR, ESI-MS spectra of **C**, **1** and **2**, Job plot, ESI-MS spectra of **2**-Fe^{3+} complex, selectivity graphs of probe **2** for Fe^{3+} ions in presence of various amino acids, BS, BSA, effect of pH on **2**-Fe^{3+} complex, and cell viability assay. See DOI: 10.1039/c2dt31316b

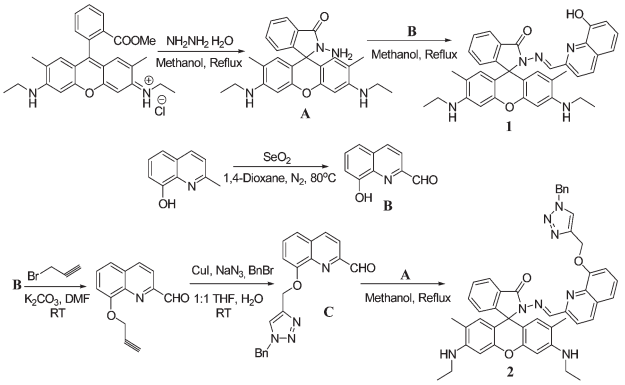

Scheme 1 Synthesis of chemosensors **1** and **2**.

Results and discussion

The rhodamine derivatives **1** and **2** containing 'O–N–N–O' and 'O–N–N–O–N' chelating moieties, respectively, were synthesized in a simple and straight forward organic synthesis procedure as shown in Scheme 1, and characterized using spectroscopic methods (Fig. S3–S8, ESI†). Although both **1** and **2** contained the rhodamine moiety, they were colourless and fluorescence inactive in both aqueous buffer [0.01 M Tris HCl–CH_3CN (pH 7.4)] and other organic solvents, presumably due to their spirocyclic ring structure. The existence of the ring-closed spirolactam as the predominant species was confirmed by the ^{13}C resonances at ~66.1 ppm, ~66.3 ppm seen in the ^{13}C-NMR spectrum of **1** and **2**, respectively.[17]

Metal ion selectivity and sensitivity of probes 1 and 2

The probe **1** in which the 8-hydroxyquinoline was conjugated with rhodamine offered 'O–N–N–O' chelating moiety for metal coordination. The absorbance and fluorescence characteristics of **1** were greatly affected by the addition of Fe^{3+} ions. The addition of equimolar concentration of Fe^{3+} ions to a 10 μM solution of **1** in aqueous buffer induced a bright fluorescence emission with a clear colour change from colourless to pink as shown in Fig. 1a. While the addition of other competitive metal ions like Li^+, Na^+, K^+, Mg^{2+}, Ca^{2+}, Sr^{2+}, Cr^{3+}, Mn^{2+}, Fe^{2+}, Co^{2+}, Ni^{2+}, Zn^{2+}, Cd^{2+}, Hg^{2+}, and Pb^{2+} did not show any significant enhancement in the intensity of pink colour, only the addition of Cu^{2+} ions showed pink colour albeit at low intensity (Fig. 1a). The observed preferential binding of Fe^{3+} over Cu^{2+} with probe **1** gave an indication that the 'O' atom present in hydroxy quinoline provided O–N–N–O combination of chelating moiety and played a vital role in attaining the selectivity for Fe^{3+} ions over Cu^{2+} ions. Since Fe^{3+} is a stronger hard acid as compared to Cu^{2+}, the incorporation of a hard base resulting in the O–N–N–O combination of chelating moiety would impart preferential interaction with Fe^{3+} over Cu^{2+} in accordance with the HSAB concept.

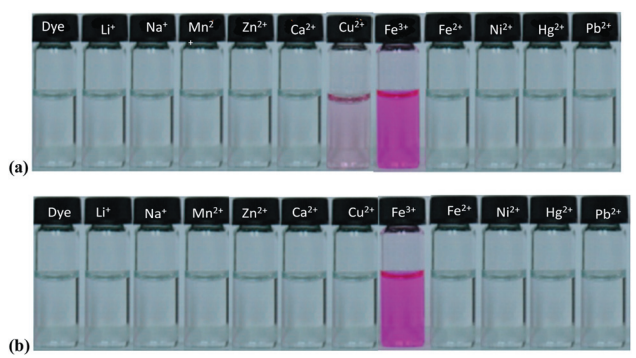

Fig. 1 Effect of addition of various metal ions (10 μM) to 10 μM solutions of fluorescent probe **1** (**a**) and fluorescent probe **2** (**b**) in 1 : 1 v/v 0.01 M Tris HCl–CH_3CN, pH 7.4.

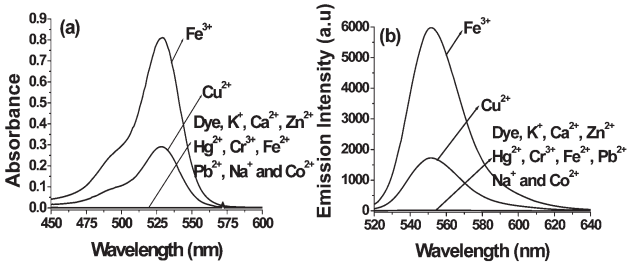

Fig. 2 Metal ion (10 μM) induced variations in the absorbance (**a**), and fluorescence (**b**) spectra of **1** (10 μM).

Th metal binding properties of **1** were further explored by using UV-Visible, and fluorescence spectroscopic techniques. A 10 μM solution of **1** in aqueous buffer (pH 7.4) showed negligible level of absorbance (Fig. 2a) and fluorescence emission (Fig. 2b) in the characteristic regions of rhodamine indicating the stability of spirolactam ring of **1** in the physiological pH condition. However, injection of Fe^{3+} ions (10 μM) led to the appearance of a broad band with two absorption maxima at ~490 and ~530 nm, arising from the xanthane moiety of rhodamine-6G (Fig. 2a). Similarly, addition of Fe^{3+} ions (10 μM) resulted in the appearance of a new band at ~552 nm in the fluorescence emission spectrum of **1** (Fig. 2b). Thus, about 617-fold enhancement in absorbance and 398-fold enhancement in fluorescence emission intensities were observed (Fig. 2) by mixing a 10 μM solution of **1** with an equimolar concentration of Fe^{3+} ions. Other competitive metal ions like Li^+, Na^+, K^+, Mg^{2+}, Ca^{2+}, Sr^{2+}, Cr^{3+}, Mn^{2+}, Fe^{2+}, Co^{2+}, Ni^{2+}, Zn^{2+}, Cd^{2+}, Hg^{2+}, and Pb^{2+} did not influence the absorption and emission behaviour of probe **1** as shown in Fig. 2. However, addition of Cu^{2+} ions (10 μM) to an equimolar solution of **1** resulted in about 221-fold increase in absorption and 114-fold increase in fluorescence emission intensities (Fig. 2). The observed preferential binding affinity of probe **1** for Fe^{3+} over Cu^{2+} ions was further confirmed from IR studies. The intensity of the band at ~1694 cm^{-1} in the IR spectrum of **1** (Fig. S9a, ESI†) corresponds to the spirolactam carbonyl streching.[18] The differential decrement in the magnitude of carbonyl band at ~1694 cm^{-1} upon addition of 0.5 equivalents of Cu^{2+} or Fe^{3+} ions clearly suggested that the interaction of probe **1** with Fe^{3+} was stronger than that observed with Cu^{2+}. These values were in good agreement with the intensity of pink colour (Fig. 1a). Therefore, the 'O–N–N–O' combination in the chelating moiety of **1** appeared to confer the preferential binding affinity for Fe^{3+} over Cu^{2+} ions.

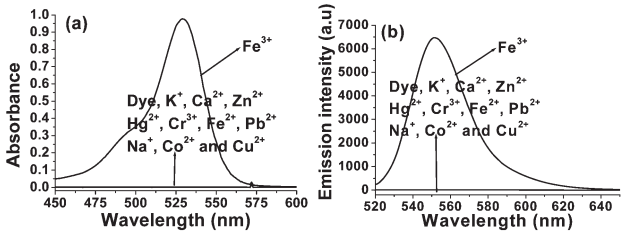

Fig. 3 Metal ion (10 μM) induced variations in the absorbance (**a**), and fluorescence (**b**) spectra of **2** (10 μM).

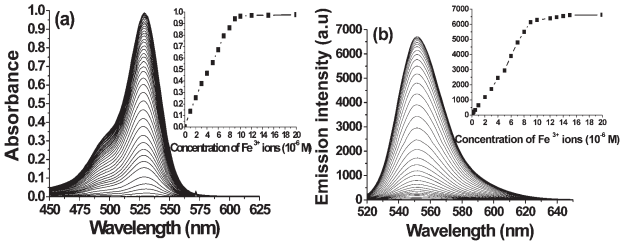

Fig. 4 Fe^{3+} concentration dependent variations in the absorbance (0–20 μM of Fe^{3+} ions) (**a**) and fluorescence (0–20 μM of Fe^{3+} ions) (**b**) spectra of **2** (10 μM).

Real-time naked-eye detection of Fe^{3+} ions using probe 2

As the 'O–N–N–O' combination in the chelating moiety of **1** displayed affinity for both Fe^{3+} and Cu^{2+} ions (Fig. 1a and 2), we reasoned that a new chemosensor with 'O–N–N–O–N' combination in the chelating moiety would provide the adequate number of coordination sites for selective complexation with Fe^{3+} ions, and be free from interference of other metal ions, including Cu^{2+} ions. Also, we reasoned that incorporation of a triazole unit to the 'O–N–N–O' combination in the chelating moiety of **1** would yield the probe **2** with 'O–N–N–O–N' combination in the chelation moiety as shown in Scheme 1. As predicted, the probe **2** was colourless in aqueous buffer, turned pink when Fe^{3+} ions were added (Fig. 1b) and did not show any interference from other metal ions including Cu^{2+}. The short response time of the probe **2** (<30 seconds) could place **2** as a real-time naked-eye chemosensor for Fe^{3+} ions.

Selectivity and sensitivity of probe 2

Negligible variations were observed in the absorbance and fluorescence characteristics of **2** (10 μM) in aqueous buffer with and without various metal ions (Fig. 3). Interestingly, addition of equimolar quantities of Cu^{2+} ions did not show any significant level of absorbance at ~530 nm (Fig. 3a) or fluorescence emission at ~552 nm (Fig. 3b), indicating the stability of the spirolactam ring of **2** in the presence of Cu^{2+} ions. However, injection of equimolar concentrations of Fe^{3+} ions led to the development of a new 744-fold intense absorption band with a maximum at ~530 nm (Fig. 3a) and a 427-fold intense fluorescence emission band with a maximum at ~552 nm (Fig. 3b) as compared to the absorbance and fluorescence properties of **2** (10 μM) in aqueous buffer without Fe^{3+} ions. Clearly, the incorporation of 'O–N–N–O–N' combination in the chelation moiety of **2** imparts selectivity for Fe^{3+} ions over other competitive metal ions including Cu^{2+} ions.

The concentration dependent variation in Fe^{3+} induced absorbance characteristics of **2** (Fig. 4a) indicated that the addition of as low as 0.1 μM concentration of Fe^{3+} ions to **2** (10 μM) in aqueous buffer (pH 7.4) was enough to induce a clear absorption band ~530 nm. A similar titration to monitor the fluorescence characteristics of **2** upon addition of Fe^{3+} ions (Fig. 4b) covering a linear range from 3.0×10^{-8} to 9.0×10^{-6} M (Fig. 4b inset) revealed the limit of detection to be 5×10^{-8} M ($^{552}I_{5\times10^{-8}}/^{552}I_0 = 3.77$).[12] It is imperative to note that the limit of detection (5×10^{-8} M) observed in the case of **2** was lower than those values reported for most of the rhodamine based Fe^{3+} sensors.[10] The

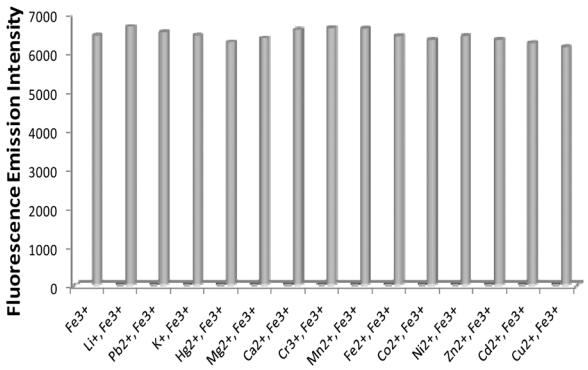

Fig. 5 Metal-ion selectivity of **2** (10 μM) in 1 : 1 v/v 0.01 M Tris HCl–CH_3CN, pH 7.4. The dark bars represent the fluorescence emission of a solution of **2** (10 μM) and 5 equiv of the cation of interest. The light bars show the fluorescence change that occurs upon addition of 1 equiv of Fe(III) to the solution containing **2** (10 μM) and the cation (50 μM).

association constant for **2**-Fe^{3+} complex was calculated using Benesi-Hildebrand plot and found to be 4.5×10^4 M^{-1}. The stoichiometry of **2**-Fe^{3+} complex was determined using Job plot (Fig. S10, ESI†) indicated that the probe **2** formed a fluorescent 1 : 1 complex with Fe^{3+} ion. The stoichiometry of the 1 : 1 complex was further confirmed from the ESI-MS data (m/z = 880–882) of **2**-Fe^{3+} complex (Fig. S11, ESI†). Further, competitive metal binding studies shown in Fig. 5, clearly established the non-interference of other metal ions (5 equivalents). Thus, probe **2** appeared to be highly sensitive and selective displaying excellent binding affinity for Fe^{3+} ions.

Furthermore, we investigated the effect of biological entities such as amino acids, blood serum (BS) and bovine serum albumin (BSA) on the sensing ability of **2**. Probe **2** (10 μM) was non-fluorescent and colourless in the presence of excess amounts (50 μM) of various amino acids. Upon addition of Fe^{3+} ions (10 μM), this colourless solution turned to pink and displayed intense fluorescence (Fig. 6), indicating the non-interference of amino acids in **2**-Fe^{3+} complex formation. Also, the fluorescence emission of **2**-Fe^{3+} complex was impassive to the addition of various amino acids (Fig. S12, ESI†), BS (Fig. S13, ESI†) and BSA (Fig. S14, ESI†). These competitive experiments revealed that the interaction of Fe^{3+} with **2** was stronger than that of Fe^{3+} with the above biological entities and the existence of the latter did not affect the detection ability of **2**.

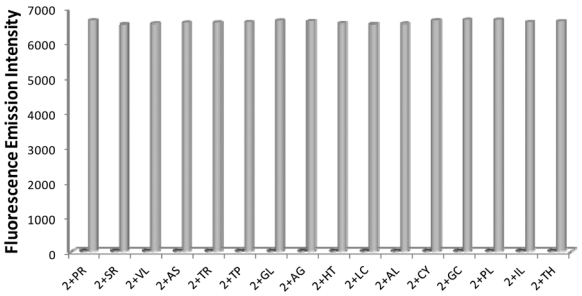

Fig. 6 Fe^{3+} ion selectivity of **2** (10 μM) in 1 : 1 v/v 0.01 M Tris HCl–CH_3CN, pH 7.4 in the presence of different amino acids. The dark bars represent the fluorescence emission of a solution of **2** (10 μM) and 5 equiv of the amino acid of interest. The light bars show the fluorescence change that occurs upon addition of Fe(III) (10 μM) to the solution containing **2** (10 μM) and the amino acid (50 μM).

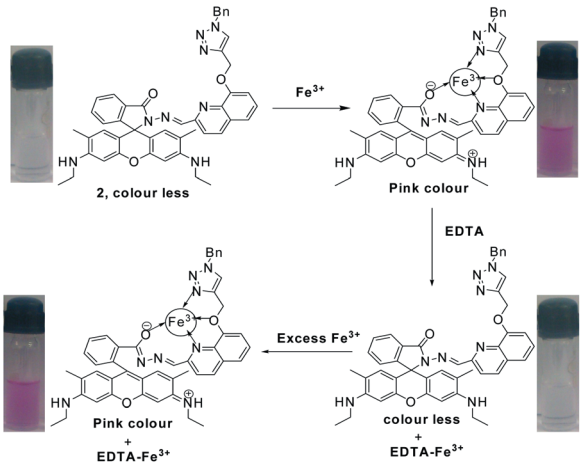

Scheme 2 Perspective binding interactions of **2** with Fe^{3+} ions.

Mechanism of Fe^{3+} ion sensing

The mechanistic aspects of Fe^{3+} ion sensing by **2** were deciphered (Scheme 2) using EDTA assay. As would be expected, binding of the hard acid Fe^{3+} to **2** resulted in enhanced absorbance and fluorescence intensities presumably due to the opening of the spirolactam ring. The Job plot and ESI-MS data (Fig. S10 and S11, ESI†) clearly confirmed the formation of a 1 : 1 complex containing two chloride ligands.[19] Further, the pink coloured solution formed by the addition of Fe^{3+} ions turned colourless upon addition of EDTA. This colourless solution regained its pink colour upon addition of an excess amount of Fe^{3+} ions. ESI-MS analysis of both colourless and pink colour solutions confirmed the interconversion between ring-closed spirolactam form and Fe^{3+} bound ring-open form of **2** (Scheme 2). Thus, the EDTA titration experiment clearly established the underlying mechanism and the fact that the colour development was due to the formation of **2**-Fe^{3+} complex and not because of any catalytic action of Fe^{3+} ions.

Effect of pH

Since the probe **2** showed Fe^{3+} induced fluorescence response in aqueous buffer (pH 7.4), the stability of **2** at various pH conditions was studied. The probe **2** was colourless in all aqueous solutions in the pH range 6–10, indicating the stability of the spirolactam ring. However, a pink colour developed in the solutions in which the pH value was below 5.0 (Fig. S15, ESI†) indicating the susceptibility of the spirolactam ring. As the pH of most biofluids is about 7.4, the observed stability of the spirolactam ring in the pH range 6–10 would make **2** suitable for bioassays.

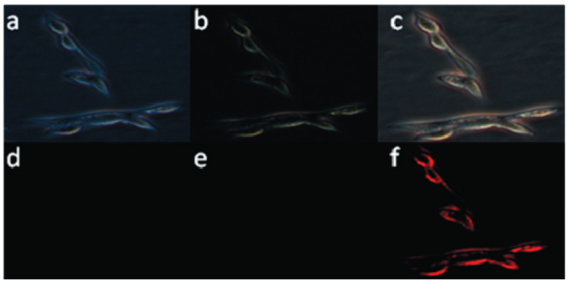

Fig. 7 Microscopic images of (**a**) untreated fibroblast cells, (**b**) cells incubated with **2** (1 μM), (**c**) cells incubated with **2** (1 μM) and Fe^{3+} (2 μM), and, fluorescence microscopic images of (**d**) untreated cells, (**e**) cells incubated with **2** (1 μM), and (**f**) cells incubated with **2** (1 μM) and Fe^{3+} (2 μM).

Detection, imaging and viability of live cells

The selective binding with Fe^{3+} ions, high sensitivity, stability at physiological pH conditions and non-interference of amino acids, blood serum and BSA in the detection process, prompted us to use the probe **2** for the detection of contaminant Fe^{3+} ions on live mouse fibroblast cells. Mouse fibroblast cell line NIH 3T3 incubated with Fe^{3+} ions (2 μM) in Dulbecco's Modified Eagle Medium (DMEM) for 2 min at 37 °C, was washed with PBS buffer (pH 7.4) to remove excess metal ions. The cells were then treated with **2** (1 μM) in the DMEM culture medium for 30 min at 37 °C, and washed with PBS buffer (pH 7.4) to remove unbound **2**. Fibroblast cells treated with both **2** and Fe^{3+} displayed intense red fluorescence as shown in Fig. 7f. A visual comparison of normal and fluorescence microscopic images clearly indicated that **2** could be used to detect live cells exposed to micro molar concentrations of Fe^{3+} ions. Fibroblast cells not contaminated with Fe^{3+} ions did not show any fluorescence. Further, the cytotoxicity of probe **2** assessed by performing MTT assay indicated that the cell viability was significant (~80–100%) up to ~6 μM concentration of probe **2** (Fig. 8).

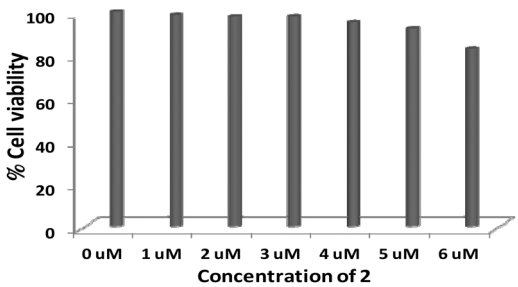

Fig. 8 The cell viability percentage of NIH 3T3 cells after treatment with different concentrations of probe **2**.

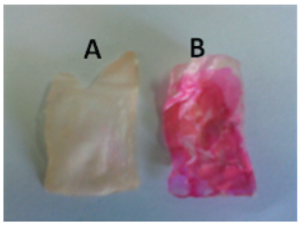

Fig. 9 Images of poly(methyl methacrylate) polymer sheets: (**A**) Doped with probe **2**; (**B**) Doped with probe **2** and sprayed with $FeCl_3$ (50 μM) solution.

Hence, at 1 μM of **2**, the concentration used for fibroblast cell imaging experiments, the probe is unlikely to be cytotoxic. These results augment the suitability of **2** for the detection and/or imaging of live cells.

Polymer thin films for Fe^{3+} sensing

Thin films of poly(methyl methacrylate) doped with **2** were prepared by dissolving the polymer (500 mg) and probe **2** (100 mg) in DCM (0.5 mL) and pouring the solution onto clean microscopic glass plates. The films formed upon air drying were removed from the glass plates and used for Fe^{3+} sensing. The films were non-fluorescent and colourless, but upon spraying a solution of $FeCl_3$ (50 μM) in acetonitrile, the colourless films turned to pink (Fig. 9). This observation opens up the possibility of designing polymer fabrics for sensing Fe^{3+} ions.

Conclusions

We have presented the synthesis of two new rhodamine 6G derivatives, **1** and **2**, containing 'O–N–NO' and 'O–N–N–O–N' combination, respectively, in the chelation moieties. The number and spatial disposition of coordinating atoms have been exploited for the selective detection of metal ions. The requirement of 'O–N–N–O–N' combination in the chelation moiety for Fe^{3+} ion selective complex formation has been demonstrated. The absence of any interference from competitive metal ions on the absorbance and fluorescence characteristics of the probe **2** in aqueous buffer has been presented as evidence for the selective detection of Fe^{3+} ions. The probe **2** is highly sensitive and forms a 1 : 1 complex with Fe^{3+} ions. The limit of detection of Fe^{3+} ions (5×10^{-8} M) observed using **2** is very much less than those values reported for rhodamine based Fe^{3+} sensors. The probe **2** is stable in the physiological pH range and non-cytotoxic up to ~6 μM. Non-interference of amino acids, human blood serum and BSA protein with the probe **2** could augment the detection and/or imaging of live cells exposed to Fe^{3+} ions. Further, the probe **2** could be formulated into a polymeric thin film sensor for Fe^{3+} detection.

Experimental

Materials and instrumentation

Dry acetonitrile and double distilled water were used in all experiments. All the materials for synthesis were purchased from commercial suppliers and used without further purification. The solutions of metal ions were prepared from the corresponding chloride salts. Absorption spectra were recorded on a Cary 50 Bio UV-visible spectrophotometer. Fluorescence measurements were performed on a Cary Eclipse fluorescence spectrophotometer. All pH measurements were made with a Systronics μpH System Model 361. NMR spectra were recorded using a Bruker Avance 400 MHz spectrometer operated at 400 MHz and a Bruker 300 MHz spectrometer operated at 300 MHz. ESI MS spectra were obtained on a PE Sciex API3000 Mass Spectrometer. Fluorescence imaging experiments were performed using a Leica DM IRB microscope equipped with EBQ-100 UV-lamp. All measurements were carried out at room temperature. Stock solutions of rhodamine derivatives (chemosensors) were prepared by dissolving 1.0 mmol of chemosensors (5.83 mg, and 7.54 mg of **1** and **2**, respectively) in 1 : 1 v/v 0.01 M Tris HCl–CH_3CN (pH 7.4) and making up to the mark in a 10 mL volumetric flask. Further dilutions were made to prepare 100 μM solutions for the experiments. Stock solutions of all amino acids (1 M) and metal ions (1 M) were prepared in de-ionized water. The blood serum was obtained *via* centrifugation of the human blood and stored at −20 °C. The serum stock solution was prepared by dissolving 50 μL of serum in 1.5 mL of PBS. The stock solution of BSA protein was prepared by dissolving 1.0 mg of BSA in 1.0 mL of PBS. Absorption and fluorescence measurements were made using a 3.0 mL cuvette. Poly(methyl methacrylate) PMMA (500 mg) and probe **2** (100 mg) were dissolved in DCM (0.5 mL), poured onto clean microscopic glass plates and air dried. The PMMA films formed were removed from the glass plates and used for Fe^{3+} sensing.

Synthesis of rhodamine 6G hydrazide A

Rhodamine 6G hydrazide was synthesized according to the reported procedure.[20]

Synthesis of triazole appended quinoline aldehyde C

The triazole appended quinoline aldehyde **C** was synthesized in a three-step procedure. To a solution of SeO_2 (1.66 g, 15 mmol) in 1,4-dixane (20 mL) under N_2 atmosphere, 2-methyl 8-quinolinol (1.59 g, 10 mmol) in 1,4-dixane (20 mL) was added dropwise, the resulted mixture was allowed to stir for 8 h under N_2 atmosphere at 70 °C and progress of the reaction was monitored by TLC. After the completion of reaction, the reaction mixture was allowed to cool to room temperature, filtered and subjected silica gel 100–200 mesh column chromatography using 95 : 5 hexane–ethylacetate as eluent to get 0.87 g (50%) of 8-hydroxyquinoline 2-aldehyde (**B**) in pure form as yellow colour solid. To a solution of 8-hydroxyquinoline 2-aldehyde (**B**) (0.87 g, 5 mmol) in DMF (20 mL) was added potassium carbonate (1.04 g, 7.5 mmol) and the solution was stirred at room temperature. Propargyl bromide (0.7 mL, 7.5 mmol) was added drop wise and the resulting mixture was allowed to stir overnight. After completion of reaction, the reaction mixture was partitioned between DCM and water, and the DCM layer was collected. The aqueous layer was extracted three times with DCM, and the combined organic extracts was dried over anhydrous

Na_2SO_4, and concentrated under vacuum to obtain the desired propargylated aldehyde that was later on converted to a triazole derivative using click chemistry. Propargylated aldehyde (0.63 g, 3 mmol) was dissolved in 1 : 1 THF/H_2O mixture and triethyl amine (0.7 mL, 5 mmol) was added. Sodium azide (0.26 g, 4 mmol), benzyl bromide (0.48 mL, 4 mmol) and cuprous iodide (*ca*.) were added to this solution. The resulting mixture was allowed to stir overnight at room temperature. Upon completion of the reaction, the mixture was filtered, extracted with ethyl acetate, concentrated under vacuum and then subjected to column chromatography to obtain the desired product. The overall yield was 0.84 g, (40%).^{1}H NMR ($CDCl_3$, 300 MHz), δ (ppm): 5.53 (2H, s, NCH_2), 5.59 (2H, s, OCH_2), 7.27 (2H, m, Ar–H), 7.37 (3H, m, Ar–H), 7.42 (1H, d, J = 9.1 Hz, Ar–H), 7.49 (1H, d, J = 7.6 Hz, Ar–H), 7.60 (1H, m, Ar–H), 7.71 (1H, s, Ar–H), 8.04 (1H, d, J = 8.3 Hz, Ar–H), 8.27 (1H, d, J = 8.3 Hz, Ar–H), 10.24 (1H, s, aldehyde-H); ESI MS: Calcd m/z 344.1; found 345.1 ($M + 1^+$).

Synthesis of rhodamine probe 1

To a solution of rhodamine 6G hydrazide **A** (0.43 g, 1 mmol) dissolved in 20 mL methanol, 8-hydroxyquinoline 2-aldehyde (**B**) (0.19 g, 1.1 mmol) was added. The red colour mixture thus obtained was refluxed in an oil bath for 3 h. After that, the solution was cooled to room temperature. The white colour precipitate formed was filtered and dried in vacuum to yield 0.47 g (80%) of **1** as colourless solid. ^{1}H NMR ($CDCl_3$, 300 MHz), δ (ppm): 1.28 (t, J = 7.2 Hz, 6H, NCH$_2CH_3$), 1.84 (s, 6H, xanthane CH_3), 3.19 (q, J = 6.9 Hz, 4H, NCH_2CH$_3$), 3.51 (s, 2H, xanthane NH), 6.39 (s, 2H, xanthene-H), 6.46 (s, 2H, xanthene-H) 7.06 (m, 2H, Ar–H), 7.16 (d, J = 7.5 Hz, 1H, Ar–H), 7.31 (m, 1H, Ar–H), 7.47 (m, 2H, Ar–H), 7.95 (d, J = 8.7 Hz, 1H, Ar–H) 8.08 (m, 2H, Ar–H) 8.47 (s, 1H, Imine–H). ^{13}C NMR ($CDCl_3$, 75 MHz), δ (ppm): 14.7, 16.7, 38.4, 66.1, 97.0, 105.8, 110.2, 117.7, 118.2, 118.8, 123.7, 123.9, 127.5, 127.7, 128.0, 128.1, 128.4, 128.4, 134.0, 135.9, 137.5, 145.4, 147.7, 151.3, 152.2, 152.3, 152.6, 165.6; ESI MS: Calcd m/z 583.3; found 584.4 ($M + 1^+$).

Synthesis of rhodamine probe 2

To a solution of rhodamine 6G hydrazide **A** (0.43 g, 1 mmol) dissolved in 20 mL methanol, triazole appended quinoline aldehyde **C** (0.38 g, 1.1 mmol) was added. The red colour mixture thus obtained was refluxed in an oil bath for 3 h. After that, the solution was cooled to room temperature. The white colour precipitate formed was filtered and dried in vacuum to yield 0.54 g (71%) of **2** as colourless solid. ^{1}H NMR ($CDCl_3$, 400 MHz), δ (ppm): 1.26 (t, J = 7.0 Hz, 6H, NCH$_2CH_3$), 1.83 (s, 6H, xanthane CH_3), 3.13 (q, J = 7.1 Hz, 4H, NCH_2CH$_3$), 3.49 (s, 2H, xanthane NH), 5.46 (s, 2H, CH_2), 5.52 (s, 2H, CH_2), 6.37 (d, J = 8.8 Hz, 4H, Xanthene-H), 7.07 (m, 1H, Ar–H), 7.18–7.34 (m, 8H, Ar–H), 7.47 (t, J = 3.6 Hz, 1H, Ar–H), 7.74 (s, 1H, triazole-H), 7.94 (d, J = 8.8 Hz, 1H, Ar–H) 8.03 (t, J = 4.1 Hz, 2H, Ar–H) 8.85 (s, 1H, Imine–H). ^{13}C NMR ($CDCl_3$, 100 MHz), δ (ppm): 14.8, 16.8, 38.4, 54.2, 63.7, 66.3, 97.0, 106.2, 111.4, 118.1, 118.9, 120.5, 123.5, 127.1, 127.5, 128.0, 128.4, 128.7, 129.1, 129.5, 133.9, 134.7, 135.9, 144.7, 147.5, 147.6, 151.5, 153.8, 165.4; ESI MS: Calcd m/z 731.4; found 732.5 ($M + 1^+$).

Acknowledgements

One of the authors, Ch. N. R, thanks the Council of Scientific and Industrial Research, New Delhi, India, for a research fellowship.

Notes and references

1 R. Meneghini, *Free Radical Biol. Med.*, 1997, **23**, 783.
2 (*a*) P. Aisen, M. Wessling-Resnick and E. A. Leibold, *Curr. Opin. Chem. Biol.*, 1999, **3**, 200; (*b*) R. S. Eisenstein, *Annu. Rev. Nutr.*, 2000, **20**, 627; (*c*) T. A. Rouault, *Nat. Chem. Biol.*, 2006, **2**, 406.
3 C. Brugnara, *Clin. Chem.*, 2003, **49**, 1573.
4 A. Ohashi, H. Ito, C. Kanai, H. Imura and K. Ohashi, *Talanta*, 2005, **65**, 525.
5 Z.-Q. Liang, C.-X. Wang, J.-X. Yang, H.-W. Gao, Y.-P. Tiang, X.-T. Tao and M.-H. Jiang, *New J. Chem.*, 2007, **31**, 906.
6 (*a*) S. Lunvongsa, M. Oshima and S. Motomizu, *Talanta*, 2006, **68**, 969; (*b*) Z. O. Tesfaldet, J. F. van Staden and R. I. Stefan, *Talanta*, 2004, **64**, 1189; (*c*) D. M. C. Gomes, M. A. Segundo, J. L. F. C. Lima and A. O. S. S. Rangel, *Talanta*, 2005, **66**, 703.
7 A. Bobrowski, K. Nowak and J. Zarebski, *Anal. Bioanal. Chem.*, 2005, **382**, 1691.
8 A. P. de Silva, H. Q. N. Gunarante, T. Gunnlaugsson, A. J. M. Huxley, C. P. McCoy, J. T. Rademacher and T. E. Rice, *Chem. Rev.*, 1997, **97**, 1515.
9 (*a*) M. Kumar, R. Kumar and V. Bhalla, *Tetrahedron Lett.*, 2010, **51**, 5559; (*b*) Z. Li, L. Zhang, X. Li, Y. Guo, Z. Ni, J. Chen, L. Wei and M. Yu, *Dyes Pigm.*, 2012, **94**, 60; (*c*) L. Zhang, J. Wang, J. Fan, K. Guo and X. Peng, *Bioorg. Med. Chem. Lett.*, 2011, **21**, 5413; (*d*) J. Yao, W. Dou, W. Qin and W. Liu, *Inorg. Chem. Commun.*, 2009, **12**, 116; (*e*) C. Queirós, A. M. G. Silva, S. C. Lopes, G. Ivanova, P. Gameiro and M. Rangel, *Dyes Pigm.*, 2012, **93**, 1447; (*f*) N. Li, Q. Xu, X. Xia, L. wang, J. Lu and X. Wen, *Mater. Chem. Phys.*, 2009, **114**, 339; (*g*) M. Zhang, Y. Gao, M. Li, M. Yu, F. Li, L. Li, M. Zhu, J. Zhang, T. Yia and C. Huanga, *Tetrahedron Lett.*, 2007, **48**, 3709; (*h*) D. Mansell, N. Rattray, L. L. Etchells, C. H. Schwalbe, A. J. Blake, E. V. Bichenkova, R. A. Bryce, C. J. Barker, A. Dıaz, C. Kremerf and S. Freeman, *Chem. Commun.*, 2008, 5161; (*i*) W. Lin, L. Yuan, J. Feng and X. Cao, *Eur. J. Org. Chem.*, 2008, 2689; (*j*) Z.-X. Li, L.-F. Zhang, W.-Y. Zhao, X.-Y. Li, Y.-K. Guo, M.-M. Yu and J.-X. Liu, *Inorg. Chem. Commun.*, 2011, **14**, 1656; (*k*) L.-J. Fan and W. E. Jones, Jr., *J. Am. Chem. Soc.*, 2006, **128**, 6784; (*l*) D. Y. Lee, N. Singh and D. O. Jang, *Tetrahedron Lett.*, 2010, **51**, 1103; (*m*) H. J. Jung, N. Singh and D. O. Jang, *Tetrahedron Lett.*, 2008, **49**, 2960; (*n*) J. Zhan, L. Wen, F. Miao, D. Tian, Xi. Zhu and H. Li, *New J. Chem.*, 2012, **36**, 656; (*o*) N. C. Lim, S. V. Pavlova and C. Bruckner, *Inorg. Chem.*, 2009, **48**, 1173; (*p*) M. Kumar, R. Kumar, V. Bhalla, P. R. Sharma, T. Kaur and Y. Qurishi, *Dalton Trans.*, 2012, **41**, 408; (*q*) H. Ouchetto, M. Dias, R. Mornet, E. Lesuissec and J.-M. Camadro, *Bioorg. Med. Chem.*, 2005, **13**, 1799; (*r*) C. Qin, Y. Cheng, L. Wang, X. Jing and F. Wang, *Macromolecules*, 2008, **41**, 7798; (*s*) A. J. Weerasinghe, C. Schmiesing, S. Varaganti, G. Ramakrishna and E. Sinn, *J. Phys. Chem. B*, 2010, **114**, 9413; (*t*) E. Hao, T. Meng, M. Zhang, W. Pang, Y. Zhou and L. Jiao, *J. Phys. Chem. A*, 2011, **115**, 8234; (*u*) W. Yina, H. Cuia, Z. Yanga, C. Li, M. She, B. Yina, J. Li, G. Zhao and Z. Shi, *Sens. Actuators, B*, 2011, **157**, 675.
10 (*a*) L. Donga, C. Wua, X. Zenga, L. Mua, S.-F. Xuea, Z. Taoa and J.-X. Zhang, *Sens. Actuators, B*, 2010, **145**, 433; (*b*) Z.-Q. Hu, Y.-C. Feng, H.-Q. Huang, L. Ding, X.-M. Wang, C.-S. Lin, M. Li and C.-P. Ma, *Sens. Actuators, B*, 2011, **156**, 428; (*c*) Y. Xiang and A. Tong, *Org. Lett.*, 2006, **8**, 1549; (*d*) X. Zhang, Y. Shiraishi and T. Hirai, *Tetrahedron Lett.*, 2008, **49**, 4178; (*e*) M. She, Z. Yang, B. Yin, J. Zhang, J. Gu, W. Yin, J. Li, G. Zhao and Z. Shi, *Dyes Pigm.*, 2012, **92**, 1337; (*f*) Z. Yang, M. She, B. Yin, J. Cui, Y. Zhang, W. Sun, J. Li and Z. Shi, *J. Org. Chem.*, 2012, **77**, 1143.
11 (*a*) J. Mao, L. Wang, W. Dou, X. Tang, Y. Yan and W. Liu, *Org. Lett.*, 2007, **9**, 4567; (*b*) M. Xu, S. Wu, F. Zeng and C. Yu, *Langmuir*, 2010,

26, 4529; (*c*) J. P. Sumner and R. Kopelman, *Analyst*, 2005, **130**, 528; (*d*) X. Zhang, Y. Shiraishi and T. Hirai, *Tetrahedron Lett.*, 2007, **48**, 5455; (*e*) N. C. Lim, S. V. Pavlova and C. Bruckner, *Inorg. Chem.*, 2009, **48**, 1173; (*f*) C. Wolf, X. Mei and H. K. Rokadia, *Tetrahedron Lett.*, 2004, **45**, 7867; (*g*) J. L. Bricks, A. Kovalchuk, C. Trieflinger, M. Nofz, M. Buschel, A. I. Tolmachev, J. Daub and K. Rurack, *J. Am. Chem. Soc.*, 2005, **127**, 13522; (*h*) Y. Ma, W. Luo, P. J. Quinn, Z. Liu and R. C. Hider, *J. Med. Chem.*, 2004, **47**, 6349; (*i*) X. Wu, B. Xu, H. Tong and L. Wang, *Macromolecules*, 2010, **43**, 8917.

12 Y. Zhao, X.-B. Zhang, Z.-X. Han, L. Qiao, C.-Y. Li, L.-X. Jian, G.-L. Shen and R.-Q. Yu, *Anal. Chem.*, 2009, **81**, 7022.

13 (*a*) Y. Chen, L. Wan, X. Yu, W. Li, Y. Bian and J. Jiang, *Org. Lett.*, 2011, **13**, 5774; (*b*) N. Jotterand, D. A. Pearce and B. Imperiali, *J. Org. Chem.*, 2001, **66**, 3224; (*c*) Y. Zhao, Z. Lin, H. Liao, C. Duan and Q. Meng, *Inorg. Chem. Commun.*, 2006, **9**, 966; (*d*) Z. Li, P. Xi, L. Huang, G. Xie, Y. Shi, H. Liu, M. Xu, F. Chen and Z. Zeng, *Inorg. Chem. Commun.*, 2011, **14**, 1241; (*e*) H. Tian, B. Li, H. Wang, Y. Li, J. Wang, S. Zhao, J. Zhu, Q. Wang, W. Liu, X. Yaoa and Y. Tang, *J. Mater. Chem.*, 2011, **21**, 10298; (*f*) R.-M. Wang, S.-B. Huang, N. Zhao and Z.-N. Chen, *Inorg. Chem. Commun.*, 2010, **13**, 1432; (*g*) X. Jiang, B. Wang, Z. Yang, Y. Liu, T. Li and Z. Liu, *Inorg. Chem. Commun.*, 2011, **14**, 1224; (*h*) Y.-F. Cheng, D.-T. Zhao, M. Zhang, Z.-Q. Liu, Y.-F. Zhou, T.-M. Shu, F.-Y. Li, T. Yi and C.-H. Huang, *Tetrahedron Lett.*, 2006, **47**, 6413; (*i*) L. Praveen, M. L. P. Reddy and R. L. Varma, *Tetrahedron Lett.*, 2010, **51**, 6626; (*j*) G. Farruggia, S. Iotti, L. Prodi, M. Montalti, N. Zaccheroni, P. B. Savage, V. Trapani, P. Sale and F. I. Wolf, *J. Am. Chem. Soc.*, 2006, **128**, 344; (*k*) L. Praveen, C. H. Suresh, M. L. P. Reddy and R. L. Varma, *Tetrahedron Lett.*, 2011, **52**, 4730; (*l*) K. Huang, H. Yang, Z. Zhou, M. Yu, F. Li, X. Gao, T. Yi and C. Huang, *Org. Lett.*, 2008, **10**, 2557; (*m*) L. Xue, Q. Liu and H. Jiang, *Org. Lett.*, 2009, **11**, 3454; (*n*) X.-L. Tang, X.-H. Peng, W. Dou, J. Mao, J.-R. Zheng, W.-W. Qin, W.-S. Liu, J. Chang and X.-J. Yao, *Org. Lett.*, 2008, **10**, 3653; (*o*) H. Yang, Z. Zhou, K. Huang, M. Yu, F. Li, T. Yi and C. Huang, *Org. Lett.*, 2007, **9**, 4729; (*p*) J. A. Gonzalez Vera, E. Lukovic and B. Imperiali, *J. Org. Chem.*, 2009, **74**, 7309; (*q*) L. Praveen, V. B. Ganga, R. Thirumalai, T. Sreeja, M. L. P. Reddy and R. L. Varma, *Inorg. Chem.*, 2007, **46**, 6277; (*r*) Y.-M. Zhang, Y. Chen, Z.-Q. Li, N. Li and Y. Liu, *Bioorg. Med. Chem.*, 2010, **18**, 1415.

14 R. W. Ramette and E. B. Sandell, *J. Am. Chem. Soc.*, 1956, **78**, 4872.

15 (*a*) L. Prodi, F. Bolletta, M. Montalti and N. Zaccheroni, *Coord. Chem. Rev.*, 2000, **205**, 59; (*b*) B. Valeur and I. Leray, *Coord. Chem. Rev.*, 2000, **205**, 3; (*c*) X. Chen, T. Pradhan, F. Wang, J. S. Kim and J. Yoon, *Chem. Rev.*, 2012, **112**, 1910; (*d*) M. Beija, C. A. M. Afonso and J. M. G. Martinho, *Chem. Soc. Rev.*, 2009, **38**, 2410; (*e*) H. N. Kim, M. H. Lee, H. J. Kim, J. S. Kim and J. Yoon, *Chem. Soc. Rev.*, 2008, **37**, 1465.

16 L. Huang, F. Chen, P. Xi, G. Xie, Z. Li, Y. Shi, M. Xu, H. Liu, Z. Ma, D. Bai and Z. Zeng, *Dyes Pigm.*, 2011, **90**, 265.

17 B. Valeur, *Molecular Fluorescence: Principles and Applications*, Wiley-VCH, Verlag GmbH, New York, 2001.

18 X. Zeng, L. Donga, C. Wua, L. Mua, S.-F. Xuea and Z. Taoa, *Sens. Actuators, B*, 2009, **141**, 506.

19 (*a*) K. Aston, N. Rath, A. Naik, U. Slomczynska, O. F. Schall and D. P. Riley, *Inorg. Chem.*, 2001, **40**, 1779; (*b*) E. C. Constable, M. S. Khan, J. Lewis, M. C. Liptrot and P. R. Raithby, *Inorg. Chim. Acta*, 1991, **181**, 207.

20 D. Wu, W. Huang, C. Duan, Z. Lin and Q. Meng, *Inorg. Chem.*, 2007, **46**, 1538.